High-Temperature Oxidation of Nickel-Based Alloys and Estimation of the Adhesion Strength of Resulting Oxide Layers

E. N. Fedorova[a,b], D. Monceau[b], D. Oquab[b], and S. A. Khudonogov[a]

[a] *Siberian Federal University, pr. Svobodnyi 79, Krasnoyarsk, 660041 Russia*

[b] *Institute Carnot, CIRIMAT INPT/UPS/CNRS, ENSIACET, Toulouse, France*

Abstract—The kinetics of isothermal oxidation (1100°C) of commercial nickel-based alloys with different content of sulfur (0.22–3.2 wt ppm) is studied. The adhesion strength in a metal/oxide system is estimated as a function of sulfur content and duration of high-temperature exposure. The scratch-test technique is proposed to quantitatively estimate the work of adhesion of resulting oxide films. It is found that the film microstructure is composed of an inner α-Al_2O_3 layer and an outer $NiAl_2O_4$ spinel layer, which are separated by discrete inclusions of TiO_2. Residual stresses in the oxide film are experimentally determined by X-ray diffraction.

DOI: 10.1134/S2070205111030051

INTRODUCTION

Heavy-duty units and components of present-day high-temperature aviation and stationary gas turbines are made of refractory single-crystal nickel alloys. To protect the surfaces of blades from gas corrosion and the impact of high operating temperatures, thermal-protective coatings (TPCs) are used. The oxidation resistance of nickel-based alloys and heat-proof coatings, as well as the lifetime of TPCs, are largely governed by the possibility of forming an α-Al_2O_3 oxide layer [1, 2], which must have an adequate strength of adhesion with a metal underlayer and the outer ceramic layer (ZrO_2–Y_2O_3) and exhibit a high resistance to thermomechanical fatigue.

The problems of adhesion strength are often associated with the presence of sulfur at the metal/oxide interface. The degree of adhesion depends on the amount of sulfur impurities in the substrate material; the content must not exceed 0.1–1 wt ppm according to the sample size [1, 3–5].

A quantitative estimation of the strength of adhesion between the resulting oxide film and the metal substrate can be carried out using the scratch-test technique [6, 7]. Results of preliminary studies showed that, to determine the work of adhesion, it is necessary to take into account the effect of residual stresses in the oxide layer. The main cause of the occurrence of residual stresses, the value of which achieves –3 to –6 GPa in a long-term operation, is temperature cycling. Upon cooling samples or real construction units, compression stresses occur in the oxide layer due to the difference in the coefficients of thermal expansion of the metal and ceramics. Thermal stresses and strains lead to the violation of integrity, a decrease in the adhesion strength of the Al_2O_3 layer, and to the acceleration of oxygen arrival to the metal surface to be protected.

The main aim of this work is to estimate the adhesion strength of the oxide layer formed upon the high-temperature oxidation of single-crystal nickel-based alloys with different concentration of sulfur. The long-term research objectives cover the determination of the adhesion strength at the metal/ceramics interface in systems with TPCs under the conditions of cyclic oxidation and the prediction of the lifetime of construction units, including blades of aviation gas turbines.

MATERIALS AND METHODS

We studied samples of French commercial first-generation nickel-based single-crystal superalloys AM1. To determine the residual stresses, we employed bulk samples of a β-NiAl single-crystal alloy modified with Pt (10 at %), which is used as an underlayer in TPC systems (Snecma-Safran Group, France). The chemical composition of AM1 is shown in Table 1. The concentration of aluminum in the studied materials is sufficient to form a continuous layer of α-Al_2O_3 during high-temperature oxidation.

AM1 alloy samples with different sulfur contents (0.22–3.2 wt ppm) are discs with diameters of 13 mm and thicknesses of 1.1–1.3 mm oriented along the [001] axis. All sample surfaces were ground using silicon carbide paper, then polished with a 1-μm diamond paste, cleaned in an ultrasonic bath in acetone and high-purity alcohol, and dried. The samples were weighed before and after oxidation using Sartorius ME and Mettler Toledo scales accurate to 0.1 mg.

Table 1. Chemical composition

Alloy/element oncentration, wt %	S (ppm)	Cr	Co	Mo	W	Ta	Al	Ti	Ni
AM1	0.22	7.5	6.5	2	5.5	8	5.3	1.2	base
	0.41								
	3.20								

Table 2. Conditions of isothermal oxidation and oxide film thickness

Alloy	Sulfur content, wt ppm	Holding under oxidation at 1100°C, h	Total film thickness*, t, μm	Thickness of inner a-Al_2O_3 layer, μm
AM1	0.22	18	1.1	~0.7
	0.41	9	1.3	~0.7
		100	2.4	~1.4
		330	3.6	~1.7
	3.2	17	1.3	~0.8
NiAlPt	–	10	0.8	~0.8

Notes: Estimated by thermogravimetric analysis data and controlled by scanning electron microscopy.

Experiments on isothermal oxidation were carried out using a SETARAM™ TAG 24S (CIRIMAT) plant, which is characterized by a high accuracy of weighing (up to 1 μg) at a temperature of 1100°C. The heating and cooling rate was 60°C/min and the storage time varied depending on the purpose of the experiment. The oxidation was performed in an atmosphere of purified air at a flow rate of 0.4 l/h.

We studied two aspects, i.e., (i) the effect of sulfur content at a constant thickness of the oxide film on the kinetics of oxidation and adhesion strength and (ii) the effect of the resulting film thickness on the adhesion strength for samples with the same chemical composition (Table 2). Samples with different sulfur content were oxidized for 9, 17, and 18 h in order to obtain a film with a comparable thickness.

The X-ray diffraction (XRD) was carried out employing SEIFERT XRD 3000 TT (CIRIMAT) and Bruker D8 ADVANCE (CIRIMAT and Siberian Federal University) instruments using $Cu_{K\alpha}$ radiation (a wavelength $K_{\alpha 1+\alpha 2} = 1.5418$ Å), a scan step of 0.02° for each sample; the recording was performed in a θ range of 10 to 40° in the θ–2θ Bragg–Brentano geometry and at fixed angles of incidence $\psi = 4$, 6, and 8°. The real-time recording of diffraction patterns during the oxidation of β-NiAlPt for determining residual stresses was carried out using a Bruker D8 Advance high-temperature diffractometer at 900 and 1100°C; the holding time was 3 and 1 h, respectively; and the rate of heating and cooling was 60°C/min.

Special software was used to process the diffraction patterns, including ANALYZE [8], CARINE Crystallography 3.1 [9], and Evaluation Package (Bruker). The structure of the resulting films was studied using LEO 435VP (CIRIMAT) scanning electron microscopes equipped with a PGT (imix-PC) system for energy dispersive spectroscopy (EDS) and a JSM 6490LV microscope (Center for Collective Use of Siberian Federal University).

To estimate the adhesion strength of the oxide film formed under conditions of high-temperature oxidation to the metal surface, we used the scratch-test technique based on a Revetest CSM Instruments device. The tests were carried out using a conical diamond indenter of the Rockwell C type with a radius of the hemispherical tip of 200 μm under the conditions of continuously increasing indentation load F_n of 1–100 N. The loading rate was 50 N/min, and the scratch length was 3 mm. The device is equipped with a built-in optical microscope, a system for monitoring the intensity of acoustic emission, and sensors of indenter penetration depth and friction force. Five scratches were made on each sample. According to optical microscopy and changes in AE signal and friction force, we determined the average value of the critical load F_{nc} (minimal) at which the first flaking of the film is observed. A schematic representation of the test is shown in Fig. 1.

RESULTS AND DISCUSSION

Isothermal Oxidation

The thermogravimetric analysis data for the isothermal oxidation of the AM1 samples are shown in Fig. 2. A high rate of oxidation is observed for all samples in the initial, so-called "transition," region. After

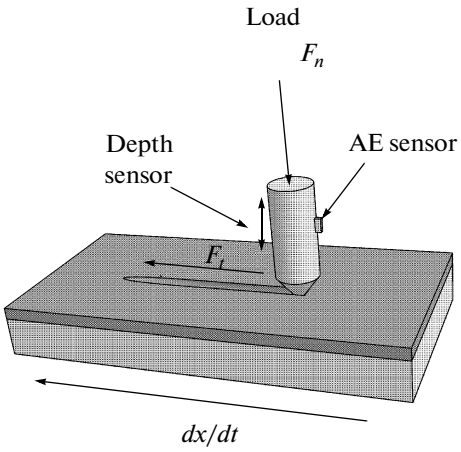

Fig. 1. Scratch-test pattern.

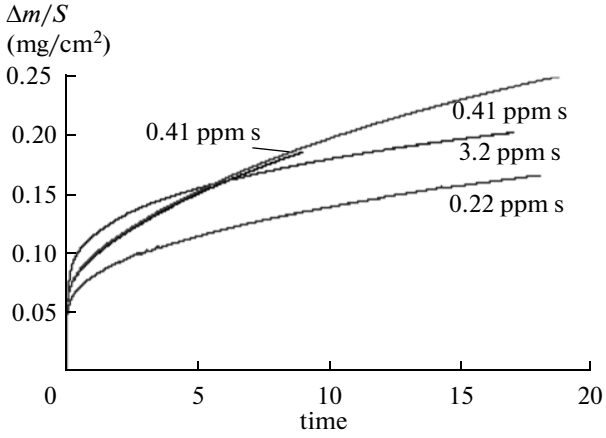

Fig. 2. Kinetics of isothermal oxidation of AM1 alloy with different sulfur concentration (ignoring mass variation during heating).

approximately 6 h of storage, the kinetics of oxidation for all samples obeys a parabolic law. The results of experiments on the isothermal oxidation have good reproducibility. As an example, Fig. 2 depicts two curves for the composition of 0.41 ppm S. The parabolic rate constant k_p for the oxide film growth was determined by approximating the parabolic law

$$t = A + B(\Delta m/S) + (1/k_p)(\Delta m/S)^2,$$

where t is the time, $\Delta m/S$ is the ratio of change in the sample weight to the surface area, and A and B are constants [10]. The values of k_p for samples with different sulfur content are listed in Table 3. Figure 2 and Table 3 show that the kinetics of oxidation of the AM1 samples is not a specific function of sulfur concentration. The highest rate of oxidation is characteristic of samples with an intermediate sulfur content of 0.41 ppm S, which can also be explained by some differences in the production of original materials or by the presence of unregulated impurities in the original rod. The authors do not yet have accurate data about these impurities. Experiments on the oxidation of samples with different surface roughness were also carried out. No significant effect of the degree of surface treatment on the kinetics of oxidation was found. The results were reported in [11].

Resulting Film Microstructure

The results of studies using a scanning electron microscope revealed that, after isothermal oxidation at 1100°C for 100 h, a multilayer structure is formed on the surface of the AM1 alloy. Figure 3 shows secondary and backscattered electron images of the microstructure of the oxide layer.

The EDS and XRD were used for phase identification. It is found that the oxide film consists of two layers, i.e., an inner layer from the side of the metal substrate, which is composed of oriented grains of α-Al_2O_3, and an outer layer, which comprises oriented grains of $NiAl_2O_4$ spinel. The layers are separated by discrete inclusions of tantalum and titanium oxides (bright spots in the backscattered electron image, Fig. 3a). The presence of titanium dioxide TiO_2 was confirmed by XRD. Upon the oxidation of the NiPtAl samples, a homogeneous film of α-Al_2O_3 is formed on the surface.

Estimation of Adhesion Strength

A review of theoretical models based on the approaches of linear fracture mechanics, as well as various methods for determining the adhesive strength, including the scratch-test technique, is presented in [12]. The scratch-test technique was used to

Table 3. Parabolic rate constant k_p for the oxide film growth under isothermal oxidation at $T = 1100$°C, >6 h

Sulfur content, wt ppm	Holding at 1100°C, h	$k_P \times 10^{-7}$ mg^2/cm^4/s	$B \times 10^5$ s cm^2/mg	$A \times 10^5$ s
0.22	18	1.4	–12.1	0.6
0.41	100	2.6	–11.5	1.1
	330	1.8	–18.5	2
3.2	17	1.1	–23.9	1.7

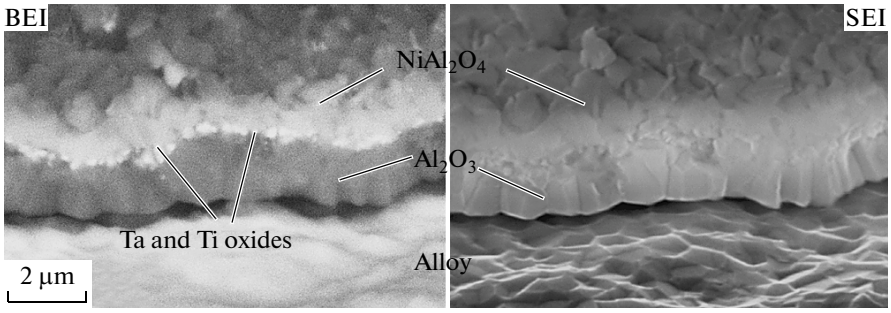

Fig. 3. SEM images of oxide film formed on surface of AM1 alloy.

measure the adhesion of various coatings on steel substrates, such as hard coatings of TiN, CrN and CrN/Cr, TiC, and/or TiC/CrC [6, 7, 13–15], as well as to estimate the adhesion strength of the Al_2O_3 layer formed during oxidation [13].

In most cases, the scratch test is used for the comparative estimation of the mechanical adhesion in systems with thin films of the same thickness on identical substrates. A quantitative estimation of adhesion strength presents some difficulties that arise due to the complex mechanical behavior of the system. The results are significantly affected by numerous factors, including the internal parameters of the system (loading rate, type and radius of the indenter) and the properties of the sample (substrate hardness, coating thickness, surface roughness, and friction coefficient). In this work, the experimental parameters were predetermined and maintained. Variables were either the sulfur content at a constant film thickness (t = const) or the film thickness with a constant chemical composition (S_{content} = const). The preliminary tests revealed that the increase in the surface roughness led to the same result for all samples, i.e., to the complexity of interpretation and the irreproducibility of results; therefore, further experiments were only carried out for polished samples (up to 1 μm). The test results are presented in Table 4.

The work of adhesion is commonly used as a measure of adhesion strength. Most theoretical models for calculating the work of adhesion are based on the Griffith energy approach, which relates the elastic strain energy with the fracture surface energy. The application of this approach for estimating the adhesion strength in a film/coating system was proposed by Laugier [16] and developed in a large body of research, including [6, 14, 15].

The models of Burnett, Rickerby, and Bull [6, 14], and Attar and Johanneson described below [15], which are designated as (1) and (2), respectively, were used to estimate the work of adhesion in this study. The main difference between these models lies in the method of estimation of local stresses.

According to (1), the expression that relates the work of adhesion W and the critical load F_{nc} is as follows:

$$W = \mu_c^2 F_{nc}^2 \frac{\nu_f^2 t}{2A^2 E_f}, \qquad (1)$$

where E_f is the Young modulus of the oxide layer, ν_f is the Poisson ratio of the oxide layer, μ_c is the friction coefficient at the critical load, t is the thickness of the oxide layer, and A is the cross-sectional area of the scratch trace.

Table 4. Average* values determined from scratch tests of AM1 samples

Sulfur content, wt ppm	Film thickness	Critical load F_{nc}, H	Friction force F_{tc}, H	Friction coefficient μ_c	Trace width d_c, μm
Effect of sulfur content at t = const					
0.22	1.1	20	1.6	0.08	90
0.41	1.3	15	1.2	0.08	86
3.2	1.3	10	0.8	0.08	76
Effect of film thickness at S_{content} = const					
	1.3	15	1.2	0.08	86
0.41	2.4	12	0.9	0.07	80
	3.6	10	0.4	0.07	76

* Averaging of results of five experiments; see text for measurement error.

The area A was determined by the formula

$$A = R^2 \sin^{-1}\left(\frac{d_c}{2R}\right) - \frac{d_c}{2}\left[R^2 - \left(\frac{d_c}{2}\right)^2\right]^{1/2},$$

where d_c is the trace width at the critical load.

In the calculations according to [15], we used the following expression to estimate the work of adhesion:

$$W = \left(\frac{\nu_f \mu_c F_{nc}}{d_c}\right)^2 \frac{1}{2E_f t}. \quad (2)$$

The physicomechanical properties of the oxide film in this study were not determined and are the subject of a separate study. Therefore, we adopted the theoretical values of elastic modulus and Poisson ratio for bulk α-Al_2O_3 as follows: E_f= 380 GPa and $\nu_f = 0.24$ [17]. According to expression (1), the work of adhesion increases with growing oxide film thickness; model (2) exhibits an inverse dependence.

Our studies using the scratch-test technique confirmed the well-known fact that the mechanical behavior at the alloy/oxide interface depends on the content of sulfur; the increase in its percentage reduces the value of the work of adhesion (Table 5).

In this case, the two models show the same tendency. Samples with high concentrations of sulfur (up to 3.2 ppm) exhibit poor adhesion of the oxide layer, which is accompanied by the appearance of a broad zone of flaking throughout the scratch. As an example, Fig. 5 depicts images of fragments of the scratch trace for AM1 samples with sulfur concentrations of (a) 0.22 and (b) 3.2 ppm corresponding to the critical load. However, for all samples, the values of the work of adhesion in the case of using expression (1) are significantly lower than in the calculations by (2); for example, for a sample with a sulfur content of 0.22 ppm, the values of W are 2.2 and 21.7 J/m^2, respectively.

Note that this result agrees well with experimental data on cyclic oxidation (Fig. 5).

Thus, scratch tests can be performed in order to predict the behavior of a system under cyclic oxidation with a constant thickness of the oxide layer.

Table 5. Values of the work of adhesion for AM1 alloy samples

Sulfur content, wt ppm	Film thickness t, mm	Work of adhesion W, J m^{-2}	
		Model 1	Model 2
Effect of sulfur content at t = const			
0.22	1.1	2.2	21.7
0.41	1.3	2.0	11.4
3.2	1.3	1.8	6.5
Effect of film thickness at $S_{content}$ = const			
	1. 3	2.0	11.4
0.41	2.4	2.8	3.5
	3.6	3.9	1.8

The effect of time of isothermal oxidation (layer thickness) on the mechanical behavior at the interface is ambiguous when using the above models, which yield the opposite results. This fact is largely determined by the microstructural changes that occur with increasing time of oxidation in both the oxide film and at the metal/oxide interface.

It is noteworthy that the tendency of decreasing adhesion with increasing storage time, which is observed through expression (2), is consistent with experimental observations. Sources of errors in the determination of the work of adhesion by models (1) and (2) is the use of the theoretical values of Young modulus and Poisson ratioE_f (10%) and ν_f (up to 30%), as well as errors in measuring the trace width d_c (±5μm) and the critical load F_{nc} (10%). However, the neglect of the value of residual stresses leads to even more significant errors. The values of W ignoring residual stresses are listed in Table 5. For example, for a sample with a sulfur content of 0.22 ppm, with regard for compressive residual stresses of –4 GPa, the values of W increase to 39 and 90 J/m^2 by expressions (1) and (2), respectively. The results are discussed in more detail in [18].

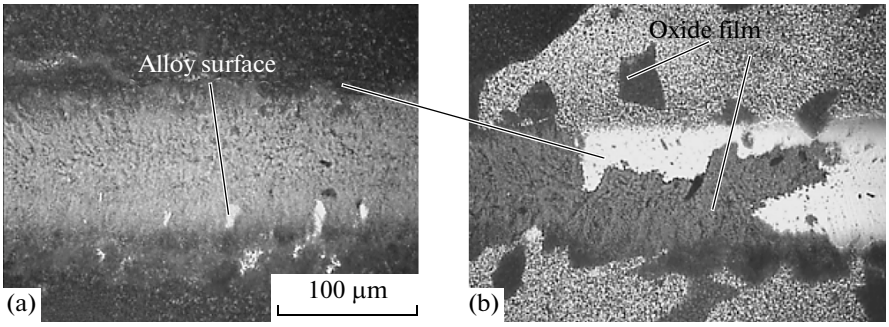

Fig. 4. Optical images of fragment of scratch trace at critical load for samples with different sulfur content (bright light areas are metal surface, dark areas are oxide film): (a) 0.22 wt ppm and (b) 3.2 wt ppm.

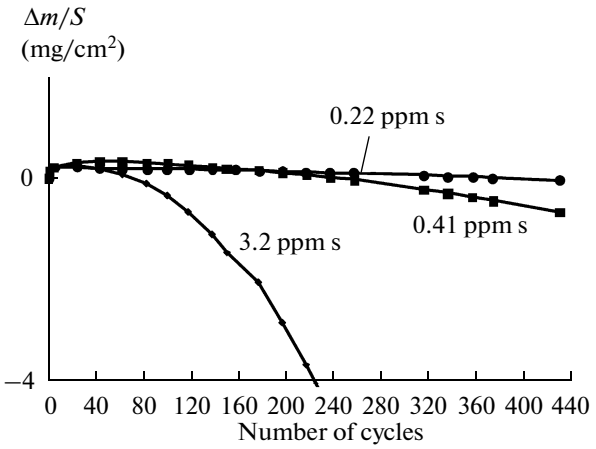

Fig. 5. Curves of cyclic oxidation of the AM1 alloy with different sulfur contents.

Residual Stresses

Experiments on the determination of residual stresses were performed by XRD for a β-NiAl sample modified with Pt; a homogeneous continuous film of α-Al_2O_3 is formed on its surface during high-temperature oxidation. The preliminary tests included the recording of diffraction patterns of reference powders of Si and α-Al_2O_3, which enable one to determine instrument errors, optimize the parameters of high-temperature experiments, and reveal the position of XRD lines of unstrained α-Al_2O_3.

The comparative analysis of the diffraction patterns showed that the XRD lines for the NiAlPt sample, on which an oxide film is formed during high-temperature oxidation, are shifted by $2\theta = 0.15$–$0.2°$ compared to the reference sample. The estimation of stresses by the technique described in [19, 20] showed that this shift corresponds to compressive stresses of 1.5–2.5 GPa, respectively. The error of the method is 20%.

We also determined the value of thermal residual stresses in the oxide film with neglect of the film growth stresses and the temperature dependence of the material characteristics by the formula proposed by the authors of [21]:

$$\sigma_T = \frac{E_f \Delta\alpha \Delta T}{1 - \nu_f},$$

where $\Delta\alpha$ is the difference between the temperature coefficients of linear expansion of the substrate and the oxide film ($\alpha_{met} = 13.6$–14×10^{-6} C^{-1}, $\alpha_f = 8 \times 10^{-6}$ C^{-1}) and ΔT is the temperature range of 1100°C–20°C. The compressive stresses were ~3 GPa. According to the literature [22], the thermal residual stresses in the film, which were determined by optical fluorescence spectroscopy (OFS), were 3.3–3.5 GPa, which is consistent with the results of this study.

CONCLUSIONS

For the rapid estimation of the adhesion strength in an alloy/oxide system and prediction of the behavior of the material under cyclic oxidation, we propose a scratch-test technique. The currently available models for the quantitative estimation of adhesion in a metal/oxide system are analyzed. The effect of sulfur concentration and the thickness of the layer formed during oxidation on the value of the work of adhesion is studied. It is found that, for a constant thickness of the oxide layer, the proposed technique can be used to predict the behavior of the system under cyclic oxidation. Residual stresses are experimentally determined by XRD.

ACKNOWLEDGMENTS

This work was performed under the joint research of the Technical Institute of the Siberian Federal University (Krasnoyarsk) and the CIRIMAT (Toulouse, France).

We are grateful to A.K. Abkaryan for his participation in XRD studies and A. Frelon and D. Samelor for their assistance in the tests.

REFERENCES

1. Smith, M.A., Frazier, W.E., and Pregger, B.A., *Mater. Sci. Eng., A,* 1995, vol. 203, p. 388.
2. Tamarin, Yu.A. and Kachanov, E.B., *Novye tekhnologicheskie protsessy i nadezhnost' GTD* (New Engineering Processes and Reliability of Gas Turbine Engines), Moscow: Tsentr. Inst. Aviats. Motorostr., 2008, no. 7, p. 144.
3. Smeggil, J.G., Funkenbush, A.W., and Bornstein, N.S., *Metall. Trans. A,* 1986, vol. 17, p. 923.
4. Hou, P.Y. and Stringer, J., *Oxid. Met.,* 1992, vol. 38, no. 5/6, p. 323.
5. Smialek, J.L., *JOM,* January 2000, p. 22.
6. Burnett, P.J. and Rickerby, D.S., *Thin Solid Films,* 1988, vol. 157, p. 233.
7. Bull, S.J. and Berasetegui, E.G., *Tribol. Int.,* 2006, vol. 39, p. 99.
8. http://www.geinspectiontechnologies.com.
9. http://pros.orange.fr/carine.crystallography.
10. Monceau, D. and Pieraggi, B., *Oxid. Met.,* 1998, vol. 50, p. 477.
11. Fedorova, Å., Monceau, D., and Oquab, D, JECH 2008, 39iemes Journees d'Etudes sur la Cinetique Heterogene (JECH-39), Toulouse, 2008.
12. Volinsky, A.A., Moody, N.R., and Gerberich, W.W., *Acta Mater.,* 2002, vol. 50, p. 441.
13. Bull, S.J., *Tribol. Int.,* 1997, vol. 30, no. 7, p. 491.
14. Bull, S.J. and Rickerby, D.S., *Surf. Coat. Technol.,* 1990, vol. 42, p. 149.
15. Attar, F. and Johannesson, T., *Surf. Coat. Technol.,* 1996, vol. 78, p. 87.
16. Laugier, M.T., *Thin Solid Films,* 1984, vol. 117, p. 243.

17. Morrell, R., *Handbook of Properties of Technical and Engineering Ceramics,* London: HMSO, 1987.
18. Fedorova, E., Monceau, D., and Oquab, D., submitted for publication in *Corros. Sci.*
19. Gorelik, S.S., Rastorguev, L.N., and Skakov, Yu.A., *Rentgenograficheskii i elektronno-opticheskii analiz. Uch. posobie dlya vuzov* (X-Ray Diffraction and Electron-Optical Analysis: a Handbook for Higher Educational Institutions), Moscow: Mosk. Inst. Stali Splavov, 1994.
20. Panova, T.V., Blinov, V.I., and Kovivchak, V.S., *Opredelenie vnutrennikh napryazhenii v metallakh* (Determination of Internal Stresses in Metals), Omsk: Omsk. Gos. Univ., 2004.
21. Tien, K. and Davidson, M.J., in *Stress Effects and the Oxidation of Metals,* Cathcarted, J.V., Ed., New York: AIME, 1975, p. 200.
22. Schumann, E., Sarioglu, C., Blachere, J.R., et al., *Oxid. Met.,* 2000, vol. 53, no. 3/4, p. 259.